Structure and Dynamics of Crowns containing the Phenyldinaphthylmethane Subunit (a Three-bladed Propeller): Observations of Correlated Rotation of the Propeller Blades and Certain Ether Segments

Joyce C. Lockhart,* Martin B. McDonnell, William Clegg, and M. N. Stuart Hill
Department of Inorganic Chemistry, University of Newcastle upon Tyne, Newcastle upon Tyne, NE1 7RU

We describe some crowns (dinaphthopolyoxacycloalkanins) containing the phenyldinaphthylmethane subunit, regarded as a propeller, the aryl rings (blades) of which are fluxional, twisting about the aryl–methine bonds. This torsional propeller movement is fluxional at room temperature on the n.m.r. timescale for some crowns, with $\Delta G^{\ddagger}_{230-240}$ of *ca.* 10—11 kcal mol^{-1}, while for others (regarded as locked propellers at room temperature), $\Delta G^{\ddagger}_{380}$ is *ca.* 19 kcal mol^{-1}. Whether fluxional in solution or no, the crowns and their salt complexes commonly exhibit just one propeller isomer in the solids; *X*-ray crystal structures of one example of a crown (**4**), and one example of a salt complex (**7**), are described in this paper. Crystal data for (**4**): $C_{38}H_{40}O_8{\cdot}0.5(CH_3)_2CO$, monoclinic, space group $P2_1/n$, $a = 14.403(2)$, $b = 13.428(1)$, $c = 17.797(3)$ Å, $\beta = 93.18(1)°$, $R = 0.070$. Crystal data for (**7**): $C_{40}H_{44}O_9KNCS{\cdot}(CH_3)_2CO$, monoclinic, space group $P2_1/c$, $a = 12.721(1)$, $b = 15.197(1)$, $c = 22.038(3)$ Å, $\beta = 92.55(1)°$, $R = 0.065$. N.m.r. spectroscopic evidence in solution suggests more than one propeller isomer in solution for fluxional crowns with six oxygen donors, while for locked crowns there is only one. The single observable process (two-ring flip) for the fluxional crowns with 5 and 7 oxygen donors exchanges environments of the two differentiable naphthyl rings and phenyl edges for pairs of isomers which cannot themselves be differentiated by n.m.r. spectroscopy. A lower energy flip exchanges differentiable isomers *via* a flip of one naphthyl and one phenyl ring for the six-donor crowns. The flexing of the polyether segments in a locked propeller has been shown to be correlated with the twisting of its propeller, using a combination of dynamic n.m.r. studies with ^1H and ^2H nuclei.

In considering the mechanism of metal complexation, one must, *inter alia*, understand the dynamics of all the conformational changes of the ligand (both free and complexed) and assess the rate of these changes relative to rates of ligand and/or metal exchange. We have been interested in the mechanism of interaction between macrocycles [for example crown ethers[1] (**1**), cryptands[2] (**2**)] and alkali metal cations. Some possible steps relevant to the mechanism[3] are shown in equations (1)—(4)

$$C' \rightleftharpoons C \qquad (1)$$

$$M^+(solv) + C \rightleftharpoons MC^+ + n(solv) \qquad (2)$$

$$MC^+ \rightleftharpoons (MC'')^+ \qquad (3)$$

$$MC^+ + C' \rightleftharpoons MC'^+ + C \qquad (4)$$

where C, C′, and C″ represent different conformational forms for a free or complexed ligand.

In order to tackle these mechanistic questions, we have designed[4] a series of propeller crown ethers, of general formula (**3**), with the two-fold aims of (*i*) controlling the rate of ether flipping sterically and (*ii*) adding suitable labels for n.m.r. kinetic studies. The triarylcarbon moiety has proved to be an interesting link for use in crown macrocycles, since it can, if suitably substituted, undergo a slow flipping, which acts as a slow switch for the crown segments. In this paper, synthesis and characterisation of the ligands are described together with the *X*-ray crystal structures of a symmetrical three-bladed propeller crown, trimethoxybenzylidenedinaphthocrown-5 (**4**), and of (**7**), the potassium thiocyanate complex of its higher analogue trimethoxybenzylidenedinaphthocrown-6 (**5**).

The crowns described here, and their conformations, are of importance in establishing the extreme of fast flipping for this series of crowns and the degree of steric hindrance required to lock the propeller in solution on the n.m.r. timescale. The benzylidenedinaphtho crowns (**5**) and (**6**) and the NaNCS complex of (**6**) have already been shown[4,5] to have the propeller structure in the crystal; but each was observed as one distinct isomer of the 16 or 8 possible for their propeller skeleta.[6] Here we report on the crystal structure of (**4**), the crown-5 homologue of (**5**), and of (**7**), the KSCN salt of (**5**). The solution n.m.r. spectra of crowns (**4**), (**5**), and (**8**)—(**17**) and their salt solutions may be interpreted in terms of the isomers found in the crystal structures, and rapidly averaged mixtures of these. These structural data are the foundation on which future mechanistic

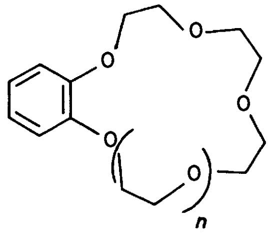

(**1**)

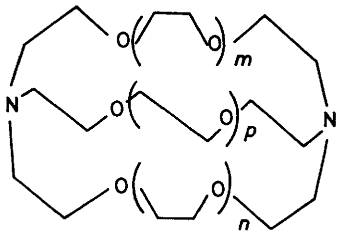

(**2**)

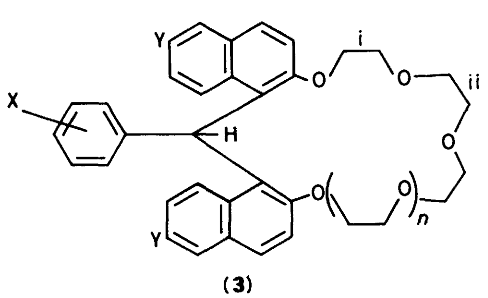

(3)

	X	Y	n
(4)	3,4,5-(OMe)$_3$	H	1
(5)	3,4,5-(OMe)$_3$	H	2
(6)	o-OMe	H	1
(8)	3,4,5-(OMe)$_3$	Bu^t	1
(9)	3,4,5-(OMe)$_3$	Bu^t	2
(10)	3,4,5-(OMe)$_3$	Bu^t	3
(11)	3,5-(CF$_3$)$_2$	H	2
(12)	2,6-Cl$_2$	H	1
(14)	p-OMe	H	1
(15)	2,6-Cl$_2$	Bu^t	1
(16)	2,6-Cl$_2$	Bu^t	2
(17)	2,6-Cl$_2$	Bu^t	3

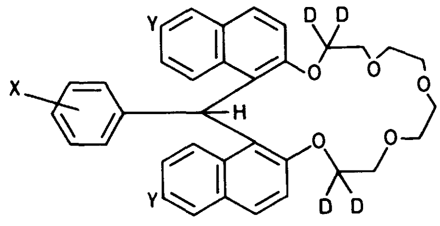

(13)

X = 2,6-(Cl$_2$) Y = H

studies of this series of propeller crown ethers may be built, and will contribute to improvements in the overall design of host molecules for a range of purposes, ranging from analytical separations to practical laboratory-scale preparations of guest ions or molecules. The curious multiple chirality[6] of the propeller fragments lends itself to the construction of larger units capable of dynamic chiral recognition, while allosteric control may be possible if each propeller unit is used as a timeswitch in a larger assembly containing several such switches.

Experimental

General Preparation of Benzylidenedinaphthols.—Various substituted benzylidenedinaphthols were prepared by the method described by Poupelin and co-workers.[7]

Preparation of 1,1′-(2,6-*Dichlorobenzylidene*)*bis*-(2-*naphthol*).—Concentrated hydrochloric acid (2 ml) was added, with stirring, to a mixture of 2-naphthol (11.5 g, 0.08 mol) and 2,6-dichlorobenzaldehyde (7.0 g, 0.04 mol) in acetic acid (60 ml). The precipitate that formed after the mixture had been left in a refrigerator for a day was filtered, washed thoroughly with water, and recrystallised from benzene to yield white crystals of 1,1′-(2,6-dichlorobenzylidene)bis-(2-naphthol) (8.2 g, 45%) (Found: M^+, 444. $C_{27}H_{18}Cl_2O_2$ requires M, 444).

Preparation of 6-*t*-*Butyl*-2-*naphthol.*—Friedel–Crafts alkylation (catalysed by anhydrous aluminium chloride) of 2-naphthol with t-butyl chloride in light petroleum afforded 6-t-butyl-2-naphthol.[8] Anhydrous aluminium chloride (10 g), 2-naphthol (80 g), t-butyl chloride (108 g), and light petroleum (300 ml) were refluxed for 5 h. After the excess of t-butyl chloride and petroleum ether had been removed, the residue was boiled with 5% aqueous sodium hydroxide (600 ml) and filtered. The cooled filtrate deposited flakes of the sodium salt of t-butylnaphthol, which were converted by hydrochloric acid into 6-t-butyl-2-naphthol, m.p. 115 °C (from light petroleum) (lit.,[8] 118—119 °C) (Found: M^+, 200. $C_{14}H_{16}O$ requires M^+, 200).

Preparation of 3,5-*Bis*(*trifluoromethyl*)*benzaldehyde.*—The substituted benzaldehydes used in the preparation of the benzylidenedinaphtho crowns were generally commercially available products. However, 3,5-bis(trifluoromethyl)benzaldehyde was prepared from 3,5-bis(trifluoromethyl)benzonitrile by Stephen reduction[9] as follows. Anhydrous stannous chloride (17.06 g, 0.09 mol) was suspended in dry diethyl ether (100 ml), which was then saturated with dry hydrogen chloride until the mixture separated into two layers, the lower viscous layer consisting of stannous chloride dissolved in ethereal hydrogen chloride. To this was added 3,5-bis(trifluoromethyl)benzonitrile (15 g, 0.06 mol) with vigorous shaking, and the mixture was left to stand for 12 h. The crystalline tin complex, which had precipitated from the solution, was removed by filtration and hydrolysed in warm water to yield a clear liquid identified as 3,5-bis(trifluoromethyl)benzaldehyde (6.2 g, 43%) (Found: M^+, 242. $C_9H_4F_6O$ requires M, 242); ν_{CO} 1 710 cm^{-1}.

Preparation of Benzylidenedinaphtho Crowns.—A satisfactory method for the triaryl crowns in this work followed one method used earlier,[5] with NaH as base in tetrahydrofuran, as described here for the preparation of 3,4,5-trimethoxybenzylidenedi-6′-t-butylnaphthocrown-7.[10]

To a solution of 1,1′-(3,4,5-trimethoxybenzylidene-6,6′-di-t-butyl)bis-(2-naphthol) (10.6 g, 0.018 mol) in dry, nitrogen-purged tetrahydrofuran (500 ml) was added NaH (80% oil dispersion; 1.65 g, 0.07 mol), followed, after 20 min of gentle reflux, by the slow addition of 1,17-bis-(p-tolylsulphonyloxy)-3,6,9,12,15-pentaoxaheptadecane (10.6 g, 0.018 mol) dissolved in tetrahydrofuran. The final mixture was refluxed for 20 h. The cooled mixture was filtered free of residual sodium salts, and the solvent was removed under reduced pressure. The brown residue was taken up in dichloromethane, extracted with water, and dried (MgSO$_4$). The mixture was treated with Celite,[10] and the dichloromethane was removed under reduced pressure. The Celite plus its absorbates was placed on the top of an alumina column (Brockman Grade IV). Gradient elution with light petroleum–diethyl ether mixtures produced a white solid; recrystallisation from 1:1 acetone–dichloromethane gave the crown (**10**) as a white powder, m.p. 204 °C. No parent ion was obtained in the mass spectrum of this compound.

Analytical Details.—The analytical and n.m.r. spectroscopic details of the benzylidenedinaphtho crowns are included in Tables 1 and 2 respectively. Electron impact-induced mass spectra of the triaryl crowns indicated a common breakdown pattern. The main fragments were the molecule ion (base peak) and fragments assigned as the xanthenium structures (**18**) and (**19**).

Thin Layer Chromatography.—Thin layer chromatography of the triaryl crowns on silica gel with diethyl ether as the solvent (containing 1% benzene), followed by development with iodine and exposure to light for a number of hours, produced coloured spots characteristic of the substitution of the phenyl rings probably due to the formation of triaryl carbenium ions.

Table 1. Analytical details of the triaryl crowns

Crown	M.p./°C	Accurate mass Found	Calc.	Found/% C	H	Calc./% C	H	Formula
(4)	200	624.2726	624.2723	72.4	6.4	73.1	6.45	$C_{38}H_{40}O_8$
(5)	183	668.3000	668.2985	71.7	6.7	71.8	6.6	$C_{40}H_{44}O_9$
(6)	208	564.2515	564.2512	76.3	6.3	76.6	6.4	$C_{36}H_{36}O_6$
(8)	241—242	736.3905	736.3975	75.1	7.5	75.0	7.7	$C_{46}H_{56}O_8$
(9)	197	780.4218	780.4237	74.1	7.8	73.8	7.7	$C_{48}H_{60}O_9$
(10)	204			73.05	7.8	72.8	7.8	$C_{50}H_{64}O_{10}$
(11)	158	714.2368	714.2416	66.0	5.1	65.5	5.1	$C_{39}H_{36}F_6O_6$
(12)	272	602.1618	602.1627	70.0	5.2	69.7	5.3	$C_{35}H_{32}Cl_2O_5$
(14)	172	564.2448	564.2512	76.6	6.4	76.6	6.4	$C_{36}H_{36}O_6$
(15)	319	714.2866	714.2879	72.2	6.8	72.2	6.8	$C_{43}H_{48}Cl_2O_5$
(16)	293	758.3085	758.3141	70.8	6.7	71.1	6.9	$C_{45}H_{52}Cl_2O_6$
(17)	265	802.3438	802.3403	70.0	6.9	70.2	7.0	$C_{47}H_{56}Cl_2O_7$

Table 2. ^{1}H N.m.r. spectroscopic details for the triaryl crowns in $CDCl_3$

	δ_H/p.p.m.				
Crown	ArH	Ar_3CH	Ether CH_2	Bu^t	Y
(4)	6.44—7.87 (14 H)	6.875	3.00—3.78 (16 H)		3.827 (3 H, OCH_3) 3.628 (6 H, OCH_3)
(5)	6.45—7.90 (14 H)	6.999	3.01—3.90 (20 H)		3.815 (3 H, OCH_3) 3.569 (6 H, OCH_3)
(6)	6.73—7.97 (16 H)	7.107	2.84—4.17 (16 H)		3.618 (3 H, OCH_3)
(8)	6.43—7.75 (12 H)	6.800	3.08—3.70 (16 H)	1.380 (18 H)	3.800 (3 H, OCH_3) 3.624 (6 H, OCH_3)
(9)	6.44—7.80 (12 H)	6.929	3.01—3.90 (20 H)	1.357 (18 H)	3.817 (3 H, OCH_3) 3.596 (6 H, OCH_3)
(10)	6.37—7.75 (12 H)	6.903	2.98—3.80 (24 H)	1.361 (18 H)	3.817 (3 H, OCH_3)
(11)	7.26—7.81 (15 H)	7.035	3.00—3.78 (20 H)		
(14)	6.66—7.90 (16 H)	6.821	2.97—3.61 (16 H)		3.610 (3 H, OCH_3)

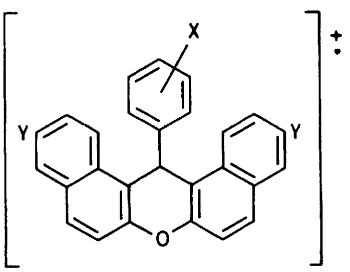

(18)

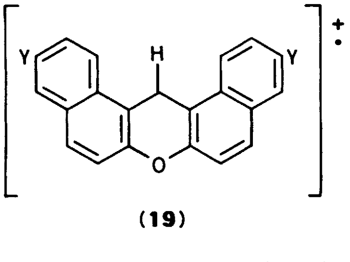

(19)

Crystal Structure Determination.—The trimethoxybenzylidine crown (4) and the crown complex (7) were both obtained as colourless crystals from solutions in 1 : 1 chloroform–acetone. Crystals were mounted on glass fibres.

All *X*-ray data were measured at 291 K with a Stoe-Siemens AED diffractometer, using graphite-monochromated Mo-K_α radiation (λ = 0.710 69 Å) and a real-time profile-fitting method for intensity estimation.[11] Cell parameters were refined from 2θ values of reflections centred at ±ω. Details are given in Table 3. Calculations were performed on a Data General

Table 3. Crystal structure determinations

	(4)	(7)
Chemical formula	$C_{38}H_{40}O_8\cdot0.5(CH_3)_2CO$	$C_{40}H_{44}O_9KNCS\cdot(CH_3)_2CO$
Formula wt.	653.8	824.0
Crystal system	Monoclinic	Monoclinic
Space group	$P2_1/n$	$P2_1/c$
a/Å	14.403(2)	12.721(1)
b/Å	13.428(1)	15.197(1)
c/Å	17.797(3)	22.038(3)
β/°	93.18(1)	92.55(1)
V/Å^3	3 436.7	4 256.2
$D_{calc.}$/g cm^{-3}	1.263	1.286
Z	4	4
F(000)/electrons	1 392	1 744
λ(Mo-K_α)/Å	0.710 69	0.710 69
μ/cm^{-1}	0.82	2.24
Crystal size/mm	0.45 × 0.50 × 0.55	0.20 × 0.55 × 0.70
Colour	Colourless	Colourless
T/°C	18	18
$2\theta_{max.}$/°	50	45
Reflections measured	6 672	5 543
Unique reflections	6 033	5 543
Reflections with $F > 4\sigma(F)$	3 973	3 442
Weighting/w^{-1}	$\sigma^2(F) + 0.000\,93F^2$	$\sigma^2(F) + 0.000\,44F^2$
Parameters refined	442	514
$R = \Sigma\lvert\Delta\rvert/\Sigma\lvert F_o\rvert$	0.070	0.065
$R_g = (\Sigma w\Delta^2/\Sigma wF_o^2)^{\frac{1}{2}}$	0.082	0.072
Max. shift/e.s.d.	0.028	0.016
Mean shift/e.s.d.	0.008	0.005
Slope of normal probability plot	1.57	1.60
Max., min. in diff. synthesis/e Å^{-3}	0.55, −0.33	0.34, −0.04

Table 4. Atomic co-ordinates (× 10^4) for compound (**4**)

	x	*y*	*z*
O(1)	948(1)	2 418(1)	3 004(1)
C(2)	1 154(3)	3 346(2)	2 664(2)
C(3)	389(3)	3 625(3)	2 116(2)
O(4)	−389(2)	3 902(2)	2 502(1)
C(5)	−1 158(3)	4 127(3)	2 007(2)
C(6)	−1 987(3)	4 276(3)	2 431(3)
O(7)	−2 275(2)	3 326(2)	2 717(2)
C(8)	−2 949(3)	3 360(3)	3 221(3)
C(9)	−3 002(3)	2 409(3)	3 626(2)
O(10)	−2 181(2)	2 230(2)	4 107(1)
C(11)	−1 507(3)	1 721(3)	3 757(2)
C(12)	−735(2)	1 490(3)	4 346(2)
O(13)	−19(1)	959(2)	4 001(1)
C(14)	−138(2)	−22(2)	3 812(2)
C(15)	446(2)	−389(2)	3 286(1)
C(16)	1 191(2)	251(2)	2 940(1)
C(17)	1 723(2)	971(2)	3 484(1)
C(18)	1 631(2)	1 990(2)	3 476(2)
C(19)	2 195(2)	2 603(3)	3 959(2)
C(20)	2 846(2)	2 206(3)	4 442(2)
C(21)	2 977(2)	1 169(3)	4 487(2)
C(22)	3 666(2)	740(3)	4 975(2)
C(23)	3 777(2)	−258(3)	5 027(2)
C(24)	3 199(2)	−889(3)	4 592(2)
C(25)	2 527(2)	−501(2)	4 097(2)
C(26)	2 395(2)	538(2)	4 013(1)
C(27)	−790(2)	−633(3)	4 155(2)
C(28)	−853(2)	−1 609(3)	3 968(2)
C(29)	−286(2)	−2 034(2)	3 429(2)
C(30)	−353(3)	−3 054(3)	3 233(2)
C(31)	188(3)	−3 459(3)	2 703(2)
C(32)	810(3)	−2 853(2)	2 351(2)
C(33)	897(2)	−1 866(2)	2 520(2)
C(34)	362(2)	−1 412(2)	3 081(1)
C(35)	896(2)	687(2)	2 177(1)
C(36)	−30(2)	844(2)	1 941(1)
C(37)	−247(2)	1 248(2)	1 234(2)
C(38)	447(2)	1 485(2)	752(1)
C(39)	1 368(2)	1 301(2)	981(2)
C(40)	1 588(2)	908(2)	1 694(2)
O(41)	−1 128(1)	1 466(2)	956(1)
C(42)	−1 881(2)	1 291(3)	1 405(2)
O(43)	229(2)	1 936(1)	71(1)
C(44)	26(3)	1 246(3)	−525(2)
O(45)	2 004(2)	1 539(2)	474(1)
C(46)	2 957(3)	1 506(4)	713(2)
X(1)	5 065(7)	9 386(6)	548(5)
X(2)[a]	5 402(12)	10 266(11)	64(10)
X(3)[a]	6 011(11)	10 693(11)	219(8)

[a] Occupancy factor = ½

ECLIPSE computer.[12] Atomic scattering factors were taken from reference 13. No absorption or extinction corrections were applied.

The structures were solved by automatic direct methods, and refined by a blocked-cascade least-squares technique with weights given by $w^{-1} = \sigma^2(F) + gF^2$, g being optimised as part of the refinement for each structure. Hydrogen atoms were included in the refinement, subject to constraints: C–H = 0.96 Å, H–C–H = 109.5°, aromatic C–H on ring external bisectors. Acetone molecules were found in both crystal structures: in the case of (**4**), these are disordered, with two half-occupied sites overlapping across an inversion centre, and no hydrogen atoms were included. There are no significant interactions between the acetone molecules and the crown or crown complex. Final atomic co-ordinates are given in Tables 4 [for (**4**)] and 5 [for (**7**)].

Table 5. Atomic co-ordinates (× 10^4) for compound (**7**)

	x	*y*	*z*
K	3 563(1)	1 846(1)	939(1)
O(1)	2 244(2)	2 058(2)	−127(1)
C(2)	1 913(4)	1 233(3)	−386(2)
C(3)	1 540(5)	650(3)	117(3)
O(4)	2 356(3)	438(2)	527(2)
C(5)	2 012(4)	−85(4)	1 012(3)
C(6)	2 967(5)	−403(4)	1 357(3)
O(7)	3 524(3)	322(2)	1 621(2)
C(8)	4 558(5)	134(4)	1 851(3)
C(9)	5 312(5)	16(4)	1 350(3)
O(10)	5 263(3)	762(2)	982(2)
C(11)	5 963(4)	806(3)	518(3)
C(12)	5 822(6)	1 622(5)	197(4)
O(13)	5 216(3)	2 113(3)	164(2)
C(14)	5 176(4)	2 927(4)	−127(2)
C(15)	4 910(4)	3 643(3)	288(2)
O(16)	3 868(2)	3 519(2)	480(1)
C(17)	3 408(3)	4 199(3)	790(2)
C(18)	2 350(3)	4 310(3)	719(2)
C(19)	1 646(3)	3 820(3)	246(2)
C(20)	2 178(3)	3 595(3)	−338(2)
C(21)	2 386(3)	2 754(3)	−522(2)
C(22)	2 817(4)	2 595(4)	−1 108(2)
C(23)	3 044(4)	3 290(5)	−1 473(2)
C(24)	2 863(4)	4 152(4)	−1 302(2)
C(25)	3 102(4)	4 866(6)	−1 689(2)
C(26)	2 909(5)	5 699(6)	−1 530(3)
C(27)	2 464(4)	5 864(4)	−976(2)
C(28)	2 237(3)	5 198(3)	−591(2)
C(29)	2 426(3)	4 303(3)	−734(2)
C(30)	4 039(4)	4 750(3)	1 177(2)
C(31)	3 593(4)	5 399(3)	1 490(2)
C(32)	2 496(3)	5 541(3)	1 456(2)
C(33)	2 016(4)	6 212(3)	1 783(2)
C(34)	955(4)	6 345(3)	1 745(2)
C(35)	335(4)	5 785(3)	1 381(2)
C(36)	765(3)	5 130(3)	1 063(2)
C(37)	1 858(3)	4 978(3)	1 072(2)
C(38)	944(3)	3 114(2)	508(2)
C(39)	55(3)	2 884(3)	155(2)
C(40)	−676(3)	2 311(3)	367(2)
C(41)	−527(3)	1 936(3)	946(2)
C(42)	361(3)	2 162(3)	1 294(2)
C(43)	1 093(3)	2 759(3)	1 079(2)
O(44)	−1 578(2)	2 056(2)	43(1)
C(45)	−1 752(3)	2 454(3)	−543(2)
O(46)	−1 252(2)	1 346(2)	1 148(1)
C(47)	−1 931(4)	1 690(4)	1 583(2)
O(48)	440(2)	1 756(2)	1 850(1)
C(49)	1 366(4)	1 878(3)	2 220(2)
N	3 872(6)	2 776(5)	2 047(3)
C(50)	4 642(7)	2 704(5)	2 276(3)
S	5 685(2)	2 661(2)	2 678(1)
O(51)	52(4)	3 561(3)	3 403(2)
C(52)	176(6)	3 953(4)	2 963(2)
C(53)	1 256(7)	4 404(4)	2 854(3)
C(54)	−593(5)	3 964(5)	2 478(3)

Solution N.M.R. Spectra.—High-resolution ^1H n.m.r. spectra were obtained on a Bruker WM-300/WB, or at 360 MHz from the S.E.R.C. High Field n.m.r. service in Edinburgh. ^{19}F Spectra were obtained on a Bruker HFX90. Second order spectra were analysed on an IBM370 computer using DNMR3[14] and NUMARIT[15] obtained from the S.E.R.C. n.m.r. program library.

Results

Two-ring Flip in Fluxional Propeller Crowns.—The ^1H n.m.r. spectra were used to follow the two-ring flip of the propeller. In

Table 6. Selected torsion angles (°) for (**4**)

C(18)–O(1)–C(2)–C(3)	173.5(3)
C(2)–C(3)–O(4)–C(5)	−177.0(3)
O(4)–C(5)–C(6)–O(7)	−71.0(4)
C(6)–O(7)–C(8)–C(9)	−164.2(3)
C(8)–C(9)–O(10)–C(11)	−90.4(4)
O(10)–C(11)–C(12)–O(13)	180.0(3)
C(12)–O(13)–C(14)–C(15)	160.9(3)
C(14)–C(15)–C(16)–C(17)	39.8(4)
C(16)–C(17)–C(18)–O(1)	7.2(4)
O(1)–C(2)–C(3)–O(4)	71.6(4)
C(3)–O(4)–C(5)–C(6)	172.1(3)
C(5)–C(6)–O(7)–C(8)	170.0(3)
O(7)–C(8)–C(9)–O(10)	67.1(4)
C(9)–O(10)–C(11)–C(12)	−174.1(3)
C(11)–C(12)–O(13)–C(14)	−74.8(4)
O(13)–C(14)–C(15)–C(16)	0.8(4)
C(15)–C(16)–C(17)–C(18)	−109.4(3)
C(17)–C(18)–O(1)–C(2)	−144.2(3)

Table 7. Selected torsion angles (°) and bond lengths (Å) for (**7**)

C(21)–O(1)–C(2)–C(3)	−165.6(4)
C(2)–C(3)–O(4)–C(5)	178.1(4)
O(4)–C(5)–C(6)–O(7)	64.2(6)
C(6)–O(7)–C(8)–C(9)	74.1(6)
C(8)–C(9)–O(10)–C(11)	175.4(4)
O(10)–C(11)–C(12)–O(13)	−17.0(13)
C(12)–O(13)–C(14)–C(15)	−126.1(8)
C(14)–C(15)–O(16)–C(17)	−169.3(4)
O(16)–C(17)–C(18)–C(19)	−9.6(6)
C(18)–C(19)–C(20)–C(21)	113.9(4)
C(20)–C(21)–O(1)–C(2)	147.3(4)
O(1)–C(2)–C(3)–O(4)	−65.2(5)
C(3)–O(4)–C(5)–C(6)	170.1(4)
C(5)–C(6)–O(7)–C(8)	−167.0(5)
O(7)–C(8)–C(9)–O(10)	54.7(6)
C(9)–O(10)–C(11)–C(12)	−178.5(5)
C(11)–C(12)–O(13)–C(14)	174.6(7)
O(13)–C(14)–C(15)–O(16)	−65.4(5)
C(15)–O(16)–C(17)–C(18)	147.8(4)
C(17)–C(18)–C(19)–C(20)	−31.6(5)
C(19)–C(20)–C(21)–O(1)	−9.1(6)

K–O(1)	2.842(3)	K–O(4)	2.764(4)
K–O(7)	2.763(4)	K–O(10)	2.717(4)
K–O(13)	2.795(5)	K–O(16)	2.769(3)
K–N	2.834(7)		

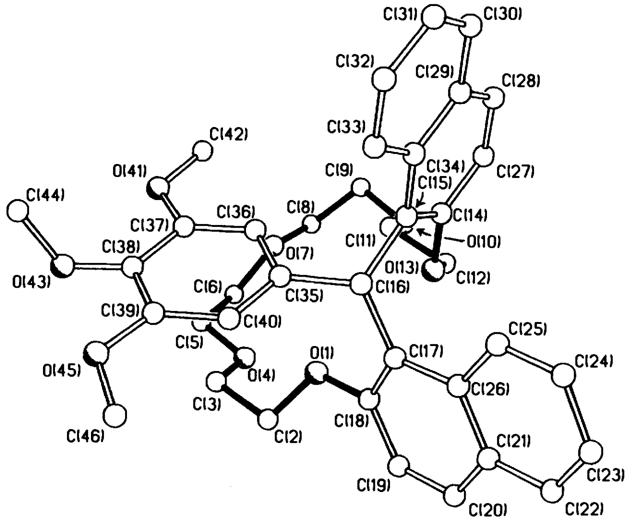

Figure 1. The structure of (**4**) showing the labelling of the atoms. Bonds are filled in the macrocyclic polyether chain, open in the propeller moiety. The view is down the H–C bond of the propeller. H Atoms are omitted

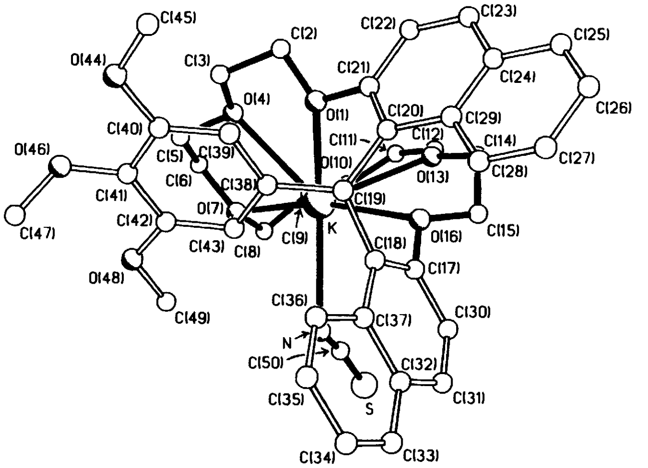

Figure 2. The structure of (**7**) showing the labelling of the atoms. Bonds are filled in the macrocyclic polyether chain and in the K co-ordination sphere, open in the propeller moiety. Other details as in Figure 1

the rigid (locked) crowns, the two naphthyl rings, the two sides of the phenyl ring, and the two sides of the ether ring are non-equivalent and are differentiable by n.m.r. spectroscopy. In fluxional crowns, these features are not distinguishable on the n.m.r. timescale. The presence of two equal-intensity Bu^t singlets was used as the criterion for a locked propeller isomer. Observation of multiple Bu^t signals of different ratios was taken to indicate the presence of more than one isomer.

3,4,5-*Trimethoxybenzylidenedi*(*t-butyl*)*naphtho Crowns*.— The trimethoxy crowns had the lowest steric barriers measured for this set of crowns. The spectra of the t-butyl-substituted crowns (**8**) and (**9**) are very similar to those of the unsubstituted ones (**4**) and (**5**) (Table 2), indicating that the t-butyl group does not affect the ring conformation, although the aromatic spectra are now simplifed and also shifted. At 300 K the ^{1}H n.m.r. spectra of each of the three t-butyl crowns (**8**)—(**10**) showed one naphthyl ABCDE spectrum, one t-butyl singlet, and one singlet for the *ortho* protons of the phenyl ring [the aromatic protons of (**8**) are shown in Figure 3a], indicating equivalence of the two naphthyl groups, the t-butyl groups, and the two edges of the phenyl ring, through rapid averaging on the n.m.r. timescale. The low-temperature behaviour is dependent on crown ether ring size.

The 300 MHz ^{1}H n.m.r. spectrum of (**8**) at 182 K in CD_2Cl_2 showed that the single t-butyl signal observed at 300 K had split into two resonances of equal integral, at 1.218 and 1.370 p.p.m. There was one methine singlet at 6.787 p.p.m. and the aromatic region (Figure 3b) showed two naphthyl ABCDE spectra. The singlet observed for the *ortho* phenyl hydrogens had split into two equal-intensity singlets at 6.211 and 6.655 p.p.m., corresponding to an AB spectrum (the *meta* coupling of less than 1 Hz was unresolved, but irradiation of one of the singlets resulted in an increase in the intensity of the other). A complete line shape analysis was made using DNMR3, of the coalescence of this AB spectrum in a series of low-temperature 90 MHz ^{1}H n.m.r. spectra of (**4**), taken in CD_2Cl_2. The activation parameters are collected in Table 8.

Table 8. Activation energy barriers ($\Delta G^{\ddagger}$) to two-ring flips in the triaryl crowns with symmetric phenyl rings

Crown	Ether oxygens	Phenyl substituent	2,3-Flip/ kcal mol^{-1}	1,2(2,1)-Flip/ kcal mol^{-1}	Mol ratio of isomers
(4)	5	3,4,5(-MeO)$_3$	11.3 (238 K)	*a*	1:0^{b}
(8)	5	3,4,5-(MeO)$_3$	*c*	*a*	1:0^{b}
(9)	6	3,4,5-(MeO)$_3$	10.9	10.5 (9.7) (210 K)	1:2^{b}
(10)	7	3,4,5-(MeO)$_3$	*c*	*a*	1:0
(11)	6	3,5-(CF$_3$)$_2$	11.6 (237 K)	10.8 (10.4) (217 K)	1:2.7^{d}
(11)•Na$^+$	6	3,5-(CF$_3$)$_2$	13.2 (261 K)	*a*	1:0^{d,e}
(13)	5	2,6-(Cl)$_2$	18.2^{f} (358 K)	*a*	1:0
(15)	5	2,6-(Cl)$_2$	18.3 (350 K)	*a*	1:0
(16)	6	2,6-(Cl)$_2$	17.9 (344 K)	*a*	1:0
(17)	7	2,6-(Cl)$_2$	17.7 (340 K)	*a*	1:0

[a] Process not observed. [b] AB Exchange (phenyl *ortho*-H). [c] Process observed but activation energy not measured. [d] CF$_3$ Exchange. [e] Solution containing excess of NaBPh$_4$. [f] iG $\rightleftharpoons$ iT D Exchange measured.

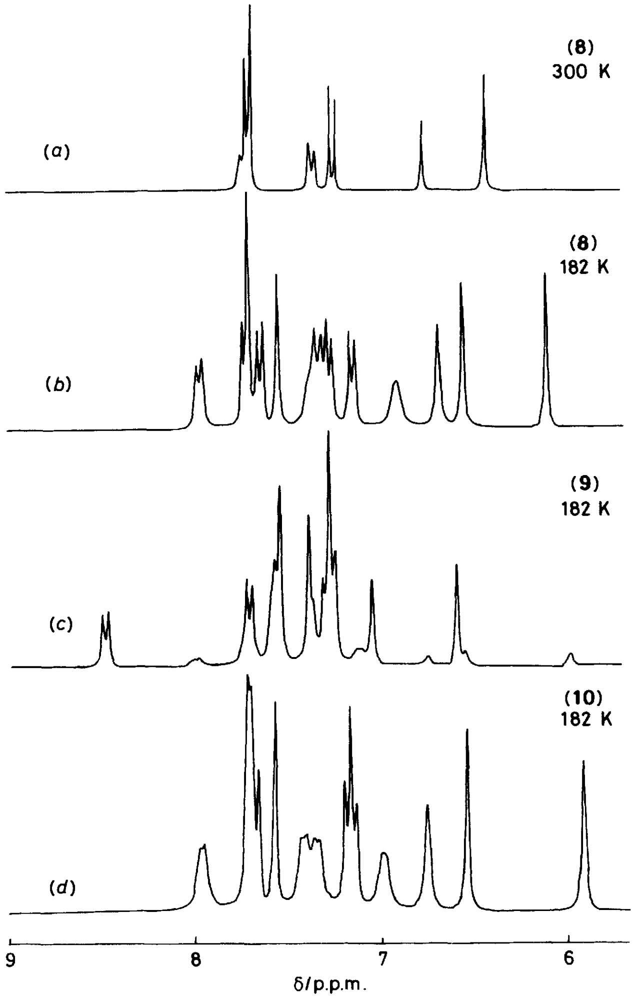

Figure 3. ^{1}H N.m.r. spectra (aromatic region) of the t-butyl-substituted trimethoxy crowns in CD$_2$Cl$_2$: (*a*) **(8)** at 300 K; (*b*) at 182 K; (*c*) **(9)** at 182 K; (*d*) **(10)** at 182 K

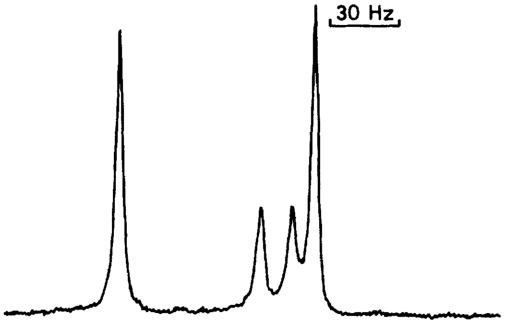

Figure 4. ^{19}F N.m.r. spectrum of **(11)** at 190 K in CD$_2$Cl$_2$–pyridine (1:1)

When a solution of the di(t-butyl)naphtho trimethoxy crown-7 **(10)** in CD$_2$Cl$_2$ was cooled to 184 K its ^{1}H n.m.r. spectrum showed a similar pattern of splitting to that observed for the crown **(8)**, with two t-butyl signals of equal intensity (separation 42 Hz), two *ortho* phenyl hydrogen singlets at 6.010 and 6.631 p.p.m., one methine singlet at 6.844 p.p.m., and two ABCDE naphthyl aromatic spectra (Figure 3d). The shift differences observed between protons on the two naphthyl rings of **(10)** compared with those for the homologue **(8)** (see Table 12) indicate the trimethoxy crown **(10)** also exists in solution as a species with a propeller skeletal isomer comparable to that observed in the crystal structure of trimethoxy crown **(4)**.

3,4,5-*Trimethoxybenzylidenedi-*(*t-butyl*)*naphtho Crown*-6 **(9)**.—The behaviour of this compound, observed by ^{1}H n.m.r. spectroscopy, resembles that of compounds **(8)** and **(10)** just described. When the mixture was cooled, the *ortho* phenyl hydrogen singlet broadened and finally split at 234 K into two broad signals, the data giving an activation energy of $\Delta G^{\ddagger}$ 10.9 ± 0.2 kcal mol^{-1}. With continued cooling these two signals did *not* sharpen but split further to produce, at 184 K, four singlets of ratio 5.8:5.8:1:1 with shifts of 7.052, 6.591, 6.547, and 5.988 p.p.m. respectively, indicative of the slowing of a second process not evident for the analogous compounds **(8)** and **(10)**. The activation energy barrier (derived using the Sharan-Atidi and Bar-Eli approximation[16] at the approximate coalescence temperature of 210 ± 2 K) from the major to minor component was $\Delta G^{\ddagger}$ 10.5 ± 0.2 kcal mol^{-1} ($\Delta G^{\ddagger}$ 9.7 ± 0.2 kcal mol^{-1} for the reverse process). The t-butyl signal had split into two lines (approximately equal-intensity singlets) at about 220 K; at 200 K these had merged again, and separate signals for the two species were not resolved. Due to the complexity of the aromatic spectrum at 184 K (see Figure 3c), a full analysis was not possible. Apart from one 8-H multiplet, the range of shifts was fairly small with a number of signals accidentally isochronous. However it was clear that two species were present, the minor component having an aromatic spectrum very similar to those of crowns **(8)** and **(10)**. Low-temperature ^{1}H n.m.r. spectroscopy of crown **(9)** in 1:1 [^{2}H$_2$]dichloromethane and [^{2}H$_5$]pyridine showed the existence, in solution, of two species of population ratio 5.4:1. Addition of excess of NaBPh$_4$ to a similar solution also showed the existence of two species at 200 K. The ratio of the populations was now 1 : 2.4. Addition of an excess of KSCN to a solution of (**9**) in CD_2Cl_2–[$^2H_5$]pyridine–CD_3OD 40 : 40 : 10 indicated a single species.

3,5-*Bis(trifluoromethyl)benzylidenedinaphtho Crown*-6 (**11**).—The CF_3 groups on the *meta* positions of the phenyl ring were selected to provide a convenient n.m.r. label, which should have negligible effect on the steric barrier to the two-ring flips. At 300 K the ^{19}F n.m.r. spectrum in CD_2Cl_2–pyridine 1 : 1 showed one sharp singlet at 62.24 p.p.m. downfield of $CFCl_3$. When cooled to 185 K the signal split into four singlets with integral ratios of 8 : 3 : 3 : 8 (Figure 4). This suggests the presence of two diastereoisomers of relative population 2.7 : 1, each having two n.m.r.-differentiable CF_3 groups. When the solution was warmed, the two upfield signals (one low and one high intensity singlet with a separation of 12 Hz at 84.69 MHz) coalesced. By 210 K this was complete and the remaining pair (one high and one low intensity singlet with a separation of 74 Hz) began to collapse. The approximate coalescence temperature of 217 ± 2 K (using the approximation of Sharan-Atidi and Bar-Eli[16]), provides activation energies for the conversion of the major to the minor diastereoisomer of $\Delta G^{\ddagger}$ 10.8 ± 0.2 kcal mol^{-1}, and $\Delta G^{\ddagger}$ 10.4 ± 0.2 kcal mol^{-1} for the reverse process. By 220 K there was one fairly sharp signal upfield with a broad signal downfield. The sharpening of the signals was not complete before a second process began the collapse of these two signals; from the approximate coalescence temperature of 237 ± 2 K an activation energy of $\Delta G^{\ddagger}$ 11.6 ± 0.2 kcal mol^{-1} is obtained. Analysis of the variable-temperature ^{19}F n.m.r. spectra by line shape analysis was not possible because the ^{19}F shift were temperature dependent.

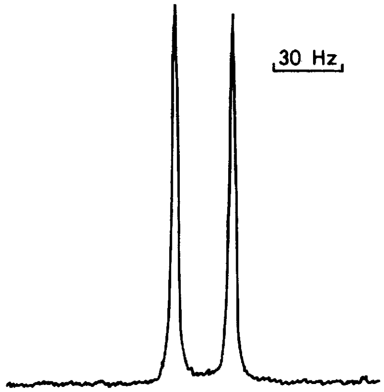

Figure 5. ^{19}F N.m.r. spectrum of (**11**) (0.03M) at 200 K with an excess of $NaBPh_4$ (0.2M) in CD_2Cl_2–pyridine (1 : 1)

Table 9. Chemical shifts[a] of segments for crowns (**13**)—(**17**)

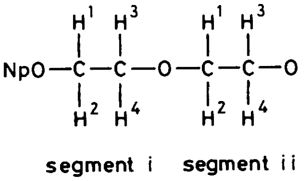

$$NpO{-}\overset{H^1}{\underset{H^2}{C}}{-}\overset{H^3}{\underset{H^4}{C}}{-}O{-}\overset{H^1}{\underset{H^2}{C}}{-}\overset{H^3}{\underset{H^4}{C}}{-}O$$

(**20**)

Segment (crown)	δ_H/p.p.m. 1	2	3	4
iG (**15**)	4.1332	2.7560	3.3687	3 4972
iG (**16**)	4.1589	3.1452	3.3272	3.4127
iG (**17**)	4.1444	3.2234	3.3169	3.4143
iT (**15**)	3.8869	3.1435	3.0049	3.5235
iT (**17**)	3.9004	2.9539	*e*	*e*
i av G,T (**14**)[b]	3.6079	3.5218	3.2345	3.0695
ii (**13**)[c]	3.8640	3.6298	3.6192	3.4805
ii (**14**)[b,d]	3.3327	3.3327	3.4007	3.4007

[a] ^1H N.m.r. spectra taken at 300 MHz in $CDCl_3$ unless otherwise stated; s.d. less than 0.0001. [b] In [$^2H_7$]Me_2NCHO and run at 360 MHz. [c] Obtained for crown deuteriated in segment i. [d] AA′BB′ Spectrum. [e] Isochronous.

Addition of an excess of $NaBPh_4$ to a solution of the crown in CD_2Cl_2–pyridine resulted in the observation of two ^{19}F singlets of equal intensity at 200 K (Figure 5), corresponding to only a single static isomer. On heating the solution, the singlets coalesced at 261 K. The two singlets showed large temperature-dependent chemical shifts, with a linear dependence of the shift separation varying from 43 Hz at 180 K to 26 Hz at 240 K; extrapolation of the shift separation–temperature graph to 261 K provided a value of 22 Hz from which an activation energy of $\Delta G^{\ddagger}$ 13.2 ± 0.1 kcal mol^{-1} was derived from exchange of the two CF_3 environments. All activation parameters are collected in Table 8.

The Two-ring Flip for Locked Propellers.—The 2,6′-dichlorophenyl propeller crowns (**12**), (**13**), and (**15**)—(**17**) gave very similar ^1H n.m.r. spectra (Tables 9 and 10), indicating the same rigid propeller isomer for each. The analogues (**12**) and (**15**) were very similar in the ether region. All five compounds had two differentiable sides at room temperature. At raised temperature, the collapse of sets of signals indicated the onset of the two-ring flip. Activation energies for the collapse of the two equal-intensity Bu^t signals were determined, as indicated in Table 8.

The Ether Rings of Locked Propellers.—A complete analysis was made (NUMARIT) of the shifts (Table 9) and coupling constants (Table 10) for many of the segments i and ii [see formula (**20**) for numbering scheme] in several of these

Table 10. Coupling constants[a] obtained for crowns (**13**)—(**17**)

Segment	Crown	$J_{1,2}$	$J_{1,3}$	$J_{1,4}$	$J_{2,3}$	$J_{2,4}$	$J_{3,4}$
iG	(**15**)	−10.72 (0.03)	2.88 (0.03)	9.59 (0.04)	2.87 (0.03)	2.85 (0.03)	−10.89 (0.04)
iG	(**16**)	−10.23 (0.03)	4.54 (0.03)	8.12 (0.02)	3.70 (0.04)	4.47 (0.02)	−10.58 (0.02)
iG	(**17**)	−10.31 (0.04)	4.53 (0.04)	7.50 (0.04)	4.37 (0.05)	4.41 (0.05)	−10.76 (0.04)
iT	(**15**)	−8.94 (0.02)	6.50 (0.03)	6.68 (0.03)	4.67 (0.02)	6.33 (0.02)	−10.14 (0.03)
iT	(**17**)	−9.69 (0.06)	4.64 (0.11)	7.38 (0.04)	4.98 (0.08)	4.55 (0.07)	*e*
iav, G,T	(**14**)[b]	−10.56 (0.02)	4.54 (0.02)	6.45 (0.02)	5.43 (0.02)	4.49 (0.02)	−10.82 (0.02)
ii	(**13**)[c]	−10.49 (0.05)	6.16 (0.05)	2.69 (0.03)	2.50 (0.07)	5.25 (0.05)	−11.25 (0.06)
ii	(**14**)[b,d]		2.66 (0.06)	6.13 (0.05)	6.13 (0.05)	2.66 (0.06)	

[a] Spectra run at 300 MHz in $CDCl_3$ unless otherwise stated; s.d. in brackets from the NUMARIT analysis. [b] In [$^2H_7$]Me_2NCHO and run at 360 MHz. [c] Obtained for crown deuteriated in segment i. [d] AA′BB′ Spectrum. *gem*-Couplings not determinable from the spectrum. [e] Not observed.

Table 11. Populations of the rotamers[a] for segment i, crowns (**14**)—(**17**)

	iG			iT		
Crown	N_g	N_g	N_t	N_g	N_g	N_t
(**15**)	0.81	0.19	0.0	0.40	0.21	0.39
(**16**)	0.61	0.21	0.18	*c*	*c*	*c*
(**17**)	0.55	0.27	0.18	0.52	0.30	0.19
(**14**)[b]	0.46	0.36	0.18			

[a] Calculated as described in ref. 20. [b] Averaged segment i present. [c] Not analysable.

Table 12. Ring current shifts[a]/Hz for crowns (**4**), (**8**), and (**10**)

Crown	(**4**)[b]	(**8**)[c]	(**10**)[d]	(**5**)[b]
H^3	13	38	10	0
H^4	4	24	42	5
H^5	9	47	42	0
H^6	50	(46)[e]	(42)[e]	1
H^7	119	129	131	11
H^8	150	191	183	24

[a] Shift differences at 300 MHz between protons in the two naphthyl rings of the crown. [b] Shift predicted from the crystal structure of (**4**) or (**5**) using the Johnson–Bovey method. [c] Shift difference in the low-temperature spectrum of (**8**). [d] Shift difference observed in the low-temperature spectrum of (**10**). [e] Separation of the 6-t-butyl signals.

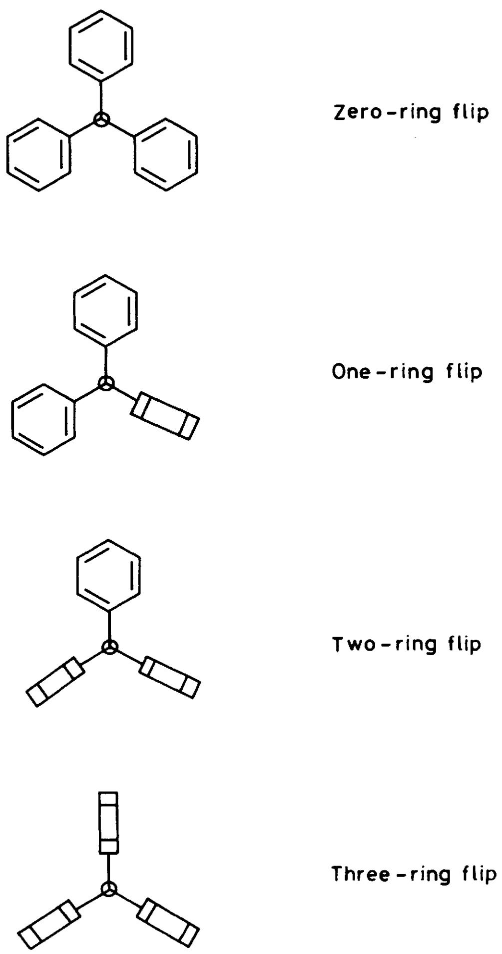

Figure 6. Idealised transition states for the four flip mechanisms for the three-bladed propellers

crowns, assisted for crown (**12**), by assignment of the ^{2}H and ^{1}H spectra of the isotopomer (**13**) substituted with deuterium in the α-positions of the segment i. From the coupling constants in Table 10, the conformer populations for segment i were estimated,*[,17] as shown in Table 11. The two differentiable segments i did not collapse completely in the ^{1}H n.m.r. spectrum for any of these compounds on heating. However, pairwise collapse of the four D{H} signals of compound (**13**) in pyridine, gave an activation energy for the symmetrisation of the ether segments i. This is shown in Table 8.

Ether Rings of Crowns with Fast Propeller Flipping.—In the ether regions, the n.m.r. spectra of such crowns were not fully averaged at room temperature. As an example the behaviour of *p*-methoxybenzylidenedinaphtho crown-5 (**14**) is described. At room temperature, the 360 MHz ^{1}H n.m.r. spectrum in [^{2}H$_7$]DMF showed rapid averaging of the propeller with one series of multiplets assigned as a naphthyl ABCDEF spectrum, another assigned as a phenyl AA′BB′ spectrum, and one methine singlet. The ether region showed a partially complete exchange process at room temperature, while at 383 K the fully averaged ether spectrum consisted of one ABCD and one AA′BB′ segment. The ABCD spectrum, due to the averaged segment i protons, was analysed in detail with NUMARIT[15] and the shifts and coupling constants are included in Tables 9 and 10.

Crystal Structures.—The crystal structure of the five-donor crown (**4**) is shown in Figure 1. Selected geometrical parameters are given in Table 6. The crystal structure showed that this crown was crystallised as a single pair of enantiomers with the same propeller skeleton as compound (**6**) and its salt, previously determined.[4] The ring tilt angles for triarylmethanes have been defined[6] relative to a reference plane formed by the three apex carbons which are joined to the methine carbon. The dihedral angle between the best plane of each aromatic ring and the reference plane is referred to as the tilt angle. The tilt angles are 51.0, 62.3, and 47.9°. The ether chain shows a sequence of g$^-$aa, g$^-$g$^+$a, ag$^-$a, ag$^+$a [proceeding from the torsion angle of the O(13)–C(12) bond along the ether strand to the torsion angle round the C(2)–O(1) bond], although the torsion angles are different from those of (**6**) (aaa, g$^+$g$^-$a, ag$^+$g$^+$, ag$^+$a) and its Na$^+$ complex (ag$^+$a, ag$^-$a, ag$^+$a, ag$^-$a). The mean diameter[18] of the ether cavity is 2.31 Å.

For compound (**7**), the KSCN complex of the six-donor trimethoxy crown (**5**), a single pair of enantiomers is again observed. The structure is shown in Figure 2, with selected geometrical parameters in Table 7. The propeller skeleton is the same as for (**4**), and differs from that found in the free crown (**5**) itself. The ether cavity has decreased from 3.90 Å in the free crown to 2.42 Å in the complex, and the torsion angle sequence is now ag$^-$a, ag$^+$a, g$^+$g$^+$a, ag$^-$a, ag$^-$a, round the ring strand reading from the torsion at the O(16)–C(15) bond to the torsion around the C(2)–O(1) bond (compared with g$^-$g$^+$a, ag$^-$g$^+$, ag$^+$a, ag$^-$a in the free crown[5]). The potassium cation is displaced from the mean oxygen plane by 0.91 Å, and the co-ordination of the potassium is completed by the nitrogen of the thiocyanate anion. The ring tilt angles for (**7**) are 54.3, 48.1, and 41.0°.

Ring Current Shift Calculations.—A comparison is made in Table 12 between the shift differences predicted for the protons

---

* The conformer populations were estimated from the observed coupling constants using the equation of Abraham and Gatti.[17]

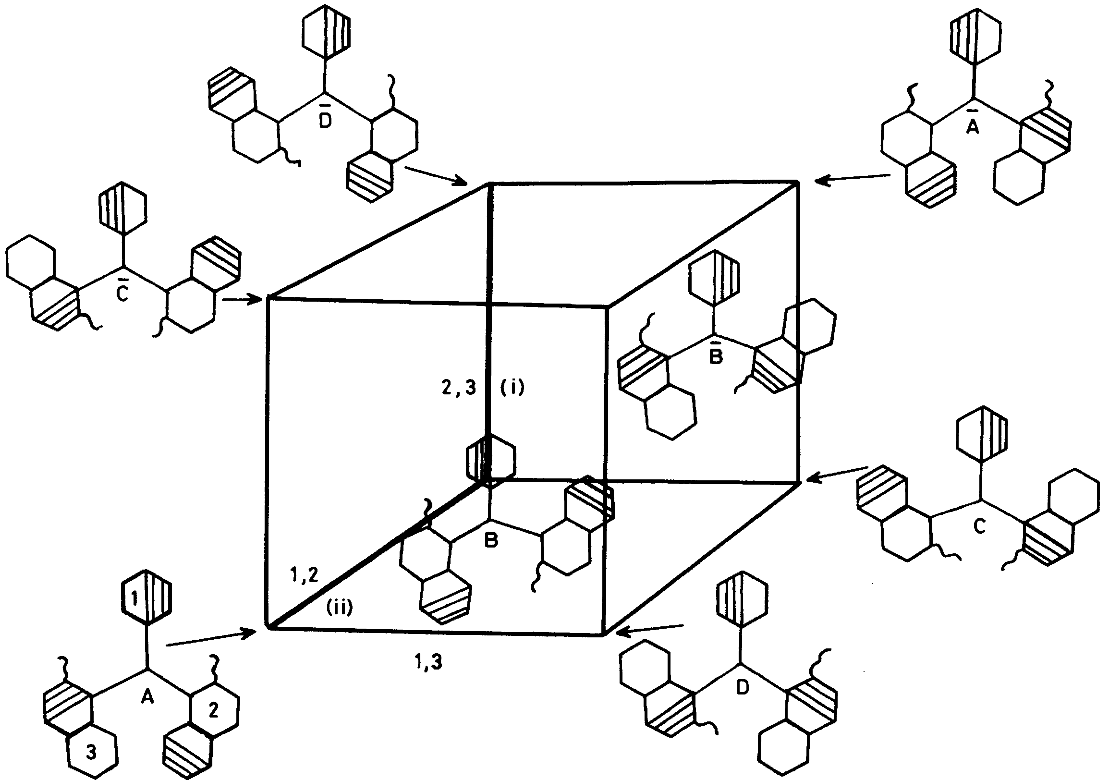

Figure 7. The eight diastereoisomers of the phenylbinaphthyl skeleton having the same chirality at the central carbon. Isomer B is that reported for compounds (**4**) and (**7**) while isomer A is that reported for compound (**5**) in ref. 5

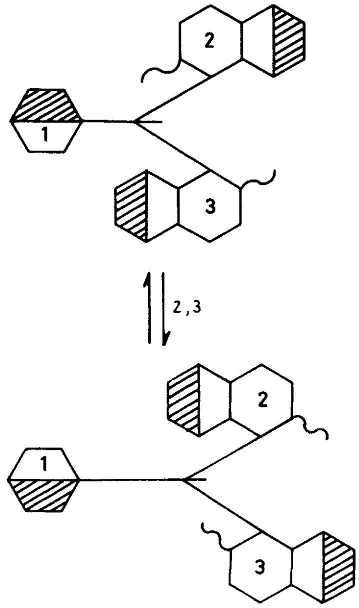

Figure 8. The 2,3 flip for isomer B, showing how the 2 and 3 rings exchange environments in the process, giving the isomer $\bar{D}$, which is of opposite helicity

on pairs of differentiable naphthyl rings on the basis of ring current calculations[19,20] based on the crystal geometry, and those observed by n.m.r. spectroscopy.

Discussion

According to Gust and Mislow,[6c] there are 32 isomers possible [16 (±) pairs] for a three-bladed propeller of the Ar_3ZX type; however degeneracies arise whenever two or more aryl groups are constitutionally identical or whenever one or more of these groups has a local C_2 axis (Table 13).

Table 13. Number of isomers for Ar_3ZX systems[a]

Number of identical rings	Number of rings with C_2 axes			
	0	1	2	3
0	32	16	8	4
2	16	8	4	2
3	8	0	0	2

[a] Taken from ref. 6[b].

Isomerism is thought to occur by correlated rotations of the aryl rings—none of the rings may move independently. Four rotational flip mechanisms were first postulated by Kurland *et al.*,[21] and investigated in great detail, especially by Mislow and co-workers.[22–32] In each of these four mechanisms, zero, one, two, or all three of the aryl rings 'flip,' *i.e.* rotate about the Ar–Z bond through planes perpendicular to the reference plane (without edge interchange) while the remaining rings rotate in the opposite direction through the reference plane (with concomitant edge interchange) (Figure 6).

Systematic empirical force field calculations,[23,24,30] and dynamic n.m.r.[22,25,27,33] studies on a variety of substituted Ar_3ZX and Ar_3Z derivatives indicate the two-ring flip as the mechanism of the lowest energy. The structure correlation method of Dunitz and co-workers has been applied to a collection of crystallographic data for Ar_3PX systems and the postulated map of the reaction path is consistent with a two-ring flip.[34]

Benzylidenedinaphtho Crowns with Symmetrically Substituted Phenyl Rings.—Crowns with symmetrically substituted phenyl rings, such as (**4**), are examples of three-bladed propellers with sixteen possible isomers of the propeller skeleton. A cube may be constructed as in the treatments given by Mislow *et al.*[6] to represent the two-ring flip paths (Figure 7) for this skeleton. The corners of the cube are intended to represent the eight possible isomers (enantiomers of those on a second cube with opposite chirality at the central chiral carbon), while the edges represent their interconversion by the two-ring flip. Isomer B has the propeller skeleton observed in the two structures presented in Figures 1 and 2, and isomer A has that found[5] in the crystal structure of (**5**). If a trigonal pyramid formed by arylmethine hydrogen and the carbons at the 4-positions of the naphthyl and phenyl rings is envisaged, then the second naphthyl rings are proximal, pointing away from the base of the pyramid, while the ether strand is distal both for (**4**) and for (**7**). In compound (**5**), one of the naphthyl rings is distal, and one end of the ether chain is proximal. The form which has usually been found in the crystal is form B.[4,5]

In the dynamic situation of rapid rotation of the OCH_2CH_2O segments, the naphthalene rings are no longer constitutionally different. In terms of the propeller fragment only eight isomers need be considered. If Figure 7 is taken to represent this situation, isomers A, B, C, and D on the lower face have the opposite helicity to $\bar{A}$, $\bar{B}$, $\bar{C}$, and $\bar{D}$ on the upper face. It can be seen that all the isomers on this cube can be interconverted by a combination of two-ring flips. The two-ring flip represented by the vertical edges of the cube causes rings 2 and 3 (marked on structure A) to flip. Consider isomer B, which has two n.m.r. differentiable naphthyl environments. It is, however, not distinguishable by n.m.r. from isomer $\bar{D}$. In a single two-ring flip (2,3-flip), which has been labelled i on the cube edge, ring 2 of B is converted into ring 3 of $\bar{D}$, and ring 3 of B into ring 2 of $\bar{D}$. This will cause the coalescence of the two sets of naphthyl signals to one. This would not be true for the other 2,3-flips. Execution of a single 1,2 or 1,3 flip on B will produce additional n.m.r.-differentiable environments. Since B is the isomer usually found in the crystal structure and can be inferred from ring current calculations (Table 12) in solution for compounds (**4**), (**8**), and (**10**), then the process observed, which interconverts pairs of naphthyl environments, is probably the 2,3 flip operating on B$\rightarrow\bar{D}$. The second process, observed for the crown-6 compounds, is probably the 1,2- (1,3-) flip which can interconvert A$\rightarrow$B. This has been labelled ii on the cube edge.

The 2,3-flip shown in Figure 8 is the only single two-ring flip which can exchange the two naphthyl rings and rotate the phenyl ring through the reference plane with edge interchange. When this becomes slow on the n.m.r. timescale, two equal-intensity butyl signals are observed, but only one methine. Slowing of the 1,2- or 1,3-flips would give a number of diastereoisomers with the resulting observation of more than one methine and a single pair of t-butyl signals, or trifluoromethyl signals *etc.* Observations of the multiplicity of the signals described in the Results section are consistent with the existence in solution of a pair of isomers which are n.m.r. equivalent for (**4**), (**8**), and (**10**). Since these two isomers are interconverted with averaging of the two naphthyl rings and averaging of the two edges of the phenyl ring, this process must be the two-ring flip labelled i. For compound (**9**), there are two observable processes: the slowing of the higher energy process produces two broad signals of equal integral which suggests it is due to a 2,3-flip. Slowing of the lower energy process gives two signals of unequal integral, and hence exchanges two differentiable isomers demonstrating the 1,2 and 1,3 flips. This information, together with predictions from crystal structure geometry, allows us to consider whether the major isomer is that observed in the crystal structure of (**5**).

Table 12 lists the predicted shift differences between the naphthyl ring protons from ring current calculations on the crystal structure (**5**). The observed spectrum of the t-butyl-substituted analogue (**9**) is thus consistent with that predicted from the crystal structure of the crown. This is further supported by the observation of accidental isochrony of the two t-butyl singlets of the major isomer. The ether region showed a very wide range of chemical shifts with multiplets of the predominant isomer between 0.5 and 5.0 p.p.m. This wide range is consistent with the arching of the ether chain over the aromatic rings observed in the published crystal structure. The signals which can be observed due to the minor isomer show good agreement with the spectra of the trimethoxy crown 5 and trimethoxy crown 7 (Figure 3c). These results are consistent with the existence in solution of two diastereoisomers, the major isomer corresponding to that observed in the crystal structure published previously, and the minor isomer corresponding to the isomer observed in the KSCN complex described in this paper [and also the same skeletal isomer described in this paper in the crystal structure of trimethoxy crown-5 (**4**)].

Correlation of the Two-ring Propeller Flip with Averaging of Segments i.—The key observation here is that the free energy of activation for the exchange of the two differentiable naphthyl rings of (**15**) in pyridine is the same within experimental error as for the exchange of segment iG and segment iT deuteriums in the $^2H\{^1H\}$ spectrum of the deuteriated isotopomer (**13**). This finding indicates that the flipping of the propeller is correlated with movement of the ether ring. However, the next section indicates that the individual segments, while restricted in movement, are not locked, but still swivelling.

Coupling Constants of the Ether Segments and the Swivelling Processes in the Ether Rings.—The coupling constants of the ether segments of the locked propeller crowns (**12**), (**13**), and (**15**)—(**17**) are not necessarily consistent with a completely static ether portion. The segments iG and iT were first analysed in detail. The magnitude of the couplings could be construed as approximating to those conjectured for one *gauche* and one *trans* segment i (as implied by our labelling G and T). However, the magnitudes are not quite right, and are more consistent with the segments still swivelling, with segment iG having only *gauche* conformers, and segment iT having a high population of *trans* conformer,[17] as indicated in Table 11. This interpretation means that the sides of the ring are differentiated by the locked propeller; the segments i are probably not completely rigid, since the *trans* population of segment iT is so high, and there is no *trans* conformer in segment iG; a reasonable interpretation would be that they can still swivel. This imparts a degree of rigidity to the locked propellers, which has been exploited elsewhere in the improvement of selectivity.[35] The segment i ether portions in the fluxional crowns [*e.g.* (**14**)] give one ABCD spectrum, indicating the two sides of the ring are equivalent. The couplings of the fluxional crown segments (average segment i) suggest approximate rotamer populations[17] in Table 13. An ABCD spectrum is observed for the average, rather than AA′BB′, since the two faces of the crown are non-equivalent even under the condition of fast propeller flipping, due to the presence of the aryl methine carbon. In the two-bladed propellers described earlier,[36] two equivalent faces, under the condition of fast propeller flipping, produced a series of AA′BB′ spectra.

An AA′BB′ spectrum was however observed for the segment ii protons of the current fluxional crowns. The shifts and coupling constants are included in Tables 9 and 10. These couplings indicate rapid interconversion between two equally populated *gauche* rotamers, typical for the usual crown segment.

Conclusion

A series of crown ethers containing a molecular propeller subunit have been synthesised. Control of switching of the two sides of the ether ring of these crowns is provided through the flipping of the propeller. The activation energy barriers ($\Delta G^{\ddagger}$) to such conformational changes have been measured for a number of crowns. A combination of ^{1}H, ^{13}C, and ^{19}F n.m.r. spectroscopy, together with *X*-ray crystallography, has shown that the propeller fragment generally occurs as a single enantiomeric pair of isomers. Crowns with 5 and 7 ether oxygens have only been found in the B form. Crowns with 6 ether oxygens show two diastereoisomeric propeller isomers (A and B in Figure 7) which can be interconverted by a series of two-ring flips. The crystal structure of free 3,4,5-trimethoxybenzylidenedinaphtho crown 6 (**5**) shows isomer A. The crystal structure of the KSCN complex of this crown shows isomer B.

In solution, the t-butyl derivative of this crown (**9**) shows both isomers at 182 K, while addition of an excess of KSCN results in the observation of a single isomer. Other 6-crowns show two isomers at low temperature, the ratio changing on complexation with alkali salts.

Acknowledgements

The authors are grateful to the S.E.R.C. for support (M. McD) and for the provision of the n.m.r. and *X*-ray diffraction facilities.

References

1 C. J. Pederson, *J. Am. Chem. Soc.*, 1967, **89**, 7107; D. J. Cram and J. M. Cram, *Acc. Chem. Res.*, 1978, **11**, 8.

2 B. Dietrich, J. M. Lehn, and J. P. Sauvage, *Tetrahedron Lett.*, 1969, 2885; J. M. Lehn, *Acc. Chem. Res.*, 1978, **11**, 49; *Pure Appl. Chem.*, 1978, **50**, 871.

3 J. C. Lockhart, 'Advances in Inorganic and Bioinorganic Mechanisms,' ed. A. G. Sykes, Academic Press, New York, 1982, vol. 1, pp. 217—268.

4 J. C. Lockhart, M. B. McDonnell, and W. Clegg, *J. Chem. Soc., Chem. Commun.*, 1984, 365.

5 W. Clegg, J. C. Lockhart, and M. B. McDonnell, *J. Chem. Soc., Perkin Trans. 2*, 1985, 1019.

6 (*a*) K. Mislow, D. Gust, P. Finocchiaro, and R. J. Boettcher, *Top. Curr. Chem.*, 1974, **47**, 1; (*b*) K. Mislow, *Acc. Chem. Res.*, 1976, **9**, 26; (*c*) D. Gust and K. Mislow, *J. Am. Chem. Soc.*, 1973, **95**, 1535.

7 J. P. Poupelin, G. Saint-Ruf, O. Foussard-Blanpin, G. Narcisse, G. Uchida-Ernouf, and R. Lacroix, *Eur. J. Med., Chem. Chim. Ther.*, 1978, **13**, 67.

8 N. P. Buu-Hoi, H. Le Bihan, F. Binon, and P. Rayet, *J. Org. Chem.*, 1950, **15**, 1060.

9 H. Stephen, *J. Chem. Soc.*, 1925, 1874.

10 J. R. Blackborow, J. C. Lockhart, D. E. Minnikin, A. C. Robson, and M. E. Thompson, *J. Chromatogr.*, 1975, **107**, 380.

11 W. Clegg, *Acta Crystallogr., Sect. A*, 1981, **37**, 22.

12 G. M. Sheldrick, 'SHELXTL: An integrated system for refining and displaying crystal structures from diffraction data,' University of Göttingen, Federal Republic of Germany, 1978.

13 'International Tables for *X*-Ray Crystallography,' Kynoch Press, Birmingham, 1974, vol. IV, pp. 99 and 149.

14 D. A. Kleier and G. Binsch, *J. Magn. Reson.*, 1971, **4**, 99.

15 J. S. Martin, A. R. Quirt, and K. M. Worvill, 'NUMARIT,' version provided by the S.E.R.C. n.m.r. program library, 1981.

16 H. Shanan-Atidi and K. H. Bar-Eli, *J. Phys. Chem.*, 1970, **74**, 961; J. Sandstrom, 'Dynamic N.M.R. Spectroscopy,' Academic Press, New York, 1982.

17 The conformer populations were estimated from the observed coupling constants using the equations of R. J. Abraham and G. Gatti, *J. Chem. Soc. B*, 1969, 961; the coupling constants for a standard OCH_2CH_2O fragment were derived from those for dioxane, J. B. Lambert, *J. Am. Chem. Soc.*, 1967, **89**, 1836.

18 K. Henrick, L. F. Lindoy, M. McPartlin, P. A. Tasker, and M. P. Wood, *J. Am. Chem. Soc.*, 1984, **106**, 1641.

19 C. E. Johnson and F. A. Bovey, *J. Chem. Phys.*, 1958, **29**, 1012.

20 S. J. Perkins, 'Biological Magnetic Resonance,' eds. L. J. Berliner and I. Reuben, Plenum Press, New York, vol. 4.

21 R. J. Kurland, I. I. Shuster, and A. K. Colter, *J. Am. Chem. Soc.*, 1965, **87**, 2279.

22 J. F. Blount, P. Finocchiaro, D. Gust, and K. Mislow, *J. Am. Chem. Soc.*, 1973, **95**, 7019.

23 P. Finocchiaro, D. Gust, and K. Mislow, *J. Am. Chem. Soc.*, 1974, **96**, 2165.

24 J. D. Andose and K. Mislow, *J. Am. Chem. Soc.*, 1974, **96**, 2168.

25 P. Finocchiaro, D. Gust, and K. Mislow, *J. Am. Chem. Soc.*, 1974, **96**, 2176.

26 P. Finocchiaro, D. Gust, and K. Mislow, *J. Am. Chem. Soc.*, 1974, **96**, 3198.

27 P. Finocchiaro, D. Gust, and K. Mislow, *J. Am. Chem. Soc.*, 1974, **96**, 3205.

28 J. P. Hummel, D. Gust, and K. Mislow, *J. Am. Chem. Soc.*, 1974, **96**, 3679.

29 M. R. Kates, J. D. Andose, P. Finocchiaro, D. Gust, and K. Mislow, *J. Am. Chem. Soc.*, 1975, **97**, 1772.

30 J. P. Hummel, E. P. Zurbach, E. N. Di Carlo, and K. Mislow, *J. Am. Chem. Soc.*, 1976, **98**, 7480.

31 K. S. Hayes, M. Nagumo, J. F. Blount, and K. Mislow, *J. Am. Chem. Soc.*, 1980, **102**, 2773.

32 R. Glaser, J. F. Blount, and K. Mislow, *J. Am. Chem. Soc.*, 1980, **102**, 2777.

33 E. E. Wille, D. S. Stephenson, P. Capriel, and G. Binsch, *J. Am. Chem. Soc.*, 1982, **104**, 405.

34 E. Bye, W. B. Schweizer, and J. Dunitz, *J. Am. Chem. Soc.*, 1982, **104**, 5893.

35 J. C. Lockhart, *J. Chem. Soc., Faraday Trans. 1*, 1986, **82**, 1161.

36 J. C. Lockhart, M. B. McDonnell, and P. D. Tyson, *J. Chem. Soc., Perkin Trans. 1*, 1983, 2153.

Received 12*th May* 1986; *Paper* 6/906